
Paper publicar[1] / *Published paper*:

Robles-Hernández, B., Sebastián, N. ; Salud, J., Diez-Berart. S., [et. al.] (2016) Molecular dynamics of a binary mixture of twist-bend nematic liquid crystal dimers studied
by dielectric spectroscopy. Physical Review E, 93. 6. 002700-1-002700-7. Doi: 10.1103/PhysRevE.93.062705

---

[1] Substituir per la citació bibliogràfica corresponent

PHYSICAL REVIEW E **00**, 002700 (2016)

Molecular dynamics of a binary mixture of twist-bend nematic liquid crystal dimers studied by dielectric spectroscopy

Beatriz Robles-Hernández,[1] Nerea Sebastián,[1,2] Josep Salud,[3] Sergio Diez-Berart,[3] David A. Dunmur,[4]
Geoffrey R. Luckhurst,[5] David O. López,[3] and M. Rosario de la Fuente[1,*]
[1] *Departamento de Física Aplicada II, Facultad de Ciencia y Tecnología, Universidad del País Vasco, Apartado 644, E-48080 Bilbao, Spain*
[2] *Otto-von-Guericke Universitat Magdeburg, Institute for Experimental Physics, ANP, 39106 Magdeburg, Germany*
[3] *Grup de Propietas Físiques dels Materials (GRPFM), Departament de Física, E.T.S.E.I.B. Universitat Politècnica de Catalunya, Diagonal 647, E-08028 Barcelona, Spain*
[4] *School of Physics and Astronomy, University of Manchester, Manchester M13 9PL, United Kingdom*
[5] *Chemistry, University of Southampton, Highfield, Southampton SO17 1BJ, United Kingdom*

(Received 23 March 2016; published xxxxxx)

We report a comprehensive dielectric characterization of a liquid crystalline binary mixture composed of the symmetric mesogenic dimer CB7CB and the nonsymmetric mesogenic dimer FFO9OCB. In addition to the high-temperature nematic phase, such a binary mixture shows a twist-bend nematic phase at room temperature which readily vitrifies on slow cooling. Changes in the conformational distribution of the dimers are reflected in the dielectric permittivity and successfully analyzed by means of an appropriate theoretical model. It is shown that the dielectric spectra of the mixture reflect the different molecular dipole properties of the components, resembling in the present case the characteristic dielectric spectra of nonsymmetric dimers. Comparison of the nematic and twist-bend nematic phases reveals that molecular dynamics are similar despite the difference in the molecular environment.

DOI: 10.1103/PhysRevE.00.002700

I. INTRODUCTION

Liquid crystal dimers consisting of two promesogenic groups joined by a flexible methylene chain containing an odd number of carbon atoms have been the focus of intense research activity over the last few years [1–15]. It was found that these compounds, of which 1″,7″-bis(4-cyanobiphenyl-4′-yl) heptane, CB7CB, is the most studied, show a first order nematic-nematic phase transition. The low-temperature nematic phase is the so-called twist-bend nematic, N_{TB}. In this phase, formed by achiral molecules, the director exhibits periodic twist and bend deformations forming a conical helix having doubly degenerate domains of opposite handedness. Although initially described for dimers of the CBnCB family, the discovery of a low temperature nematic phase boosted research in the area, and a number of materials combining different mesogenic units linked by chains have been identified which exhibit the N_{TB} phase [16–18] and its chiral counterpart [19,20]. It is now recognized that molecular curvature plays a crucial role in stabilizing the twist-bend nematic phase. For liquid crystal dimers the nature of the links between the flexible spacer composed of methylene groups and the mesogenic groups, together with the length of the spacer, play a key role. For example, methylene as opposed to ether links provides a better stabilization of the N_{TB} phase and shorter rather than longer odd spacers also tend to stabilize the phase. The low-energy gaps between the conformers generated by the flexible spacer result in a distribution of energetically favored molecular conformations, promoting a preferred bent shape for molecules having linking chains with an odd number of carbon atoms. This also causes a drastic reduction of the bend elastic constant in the conventional nematic phase [21] above the twist-bend nematic phase. According to the Landau-like theory developed by Dozov [22], the transition to the twist-bend nematic phase occurs when the bend elastic constant vanishes. However, the ultimate physical mechanism causing the director modulation remains controversial. A flexoelectric coupling between bend deformation and electric polarization [23,24] or purely elastic distortions of the director due to molecular curvature [22] are considered to be possible causes behind the formation of such twist-bend nematic deformations. Indeed Monte Carlo simulations of rigid, apolar bent molecules show that this system can still form the twist-bend nematic phase and that the transition is driven by molecular shape alone [25]. The latest theoretical approaches point towards the primary role of the molecular shape through steric interactions for the appearance of the N-N_{TB} transition [26,27].

The presence of polar groups in the mesogenic units of the dimers can be used to explore the evolution of the conformational population distribution in nematic phases through analysis of the dielectric properties of the material, and so reveal details of the structure in the twist-bend nematic phase. We have successfully employed such an approach to interpret the static and dynamic dielectric behavior of various nematic dimers, ranging from the symmetric dimers CB7CB or CB9CB [1,6] to the highly nonsymmetric CBOnO.Py dimeric family [28,29]. However, until now all dimers showing a stable N_{TB} phase and studied by dielectric spectroscopy have had identical terminal groups, and so the main motivation of this paper is to analyze the molecular orientational dynamics in the N_{TB} phase when the dimers are nonsymmetric. We have recently shown that 1″-(2′,4-difluorobiphenyl-4′-yloxy)-9″-(4-cyanobiphenyl-4′-yloxy) nonane (FFO9OCB), an ether-linked nonsymmetric odd dimer, exhibits a monotropic N_{TB} phase [30], and that in binary mixtures with CB7CB there is also a monotropic N_{TB} phase, which can be vitrified [31].

---

[*] Corresponding author: rosario.delafuente@ehu.es

This phase, although monotropic, is stable enough to allow a proper characterization. That is, the addition of a methylene-linked dimer (CB7CB) to an ether-linked dimer (FFO9OCB) enhances the stability of the twist-bend nematic phase, as expected from earlier detailed miscibility studies [31–33]. Such behavior makes these mixtures the ideal candidates for the focus of this study. The N_{TB}-N transition is always first order, regardless of the concentration of the two mesogenic compounds in the mixed systems, with a decreasing first-order transition entropy on increasing the FFO9OCB concentration [31].

In this paper we present a complete dielectric study of a mixture with a mole fraction of CB7CB equal to 0.48, having a significant proportion of the nonsymmetric component FFO9OCB, which conveniently shows a broad N_{TB} range that on further cooling becomes a glassy state [N_{TB} glass (−6 °C) N_{TB} (77 °C) N (110 °C) I]. Its static dielectric behavior and the frequency-dependent dielectric permittivity will be thoroughly examined and discussed in relation to the behavior of pure components CB7CB and FFO9OCB. As will be shown, the mixture presents a dielectric spectrum similar to that of nonsymmetric dimers with three relaxation modes in both nematic phases, which will be analyzed in the framework of the molecular theory proposed by Stocchero *et al.* [34].

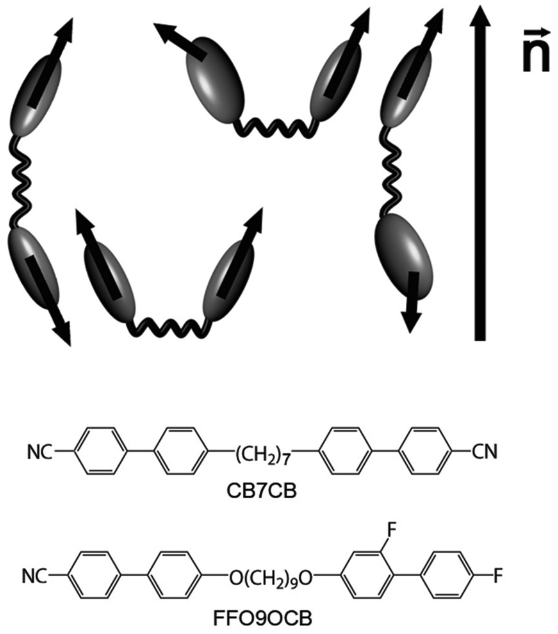

FIG. 1. Chemical structures of CB7CB and FFO9OCB. Schematic representation of the two main conformers for both dimers.

II. RESULTS AND DISCUSSION

Both pure liquid crystal dimers CB7CB and FFO9OCB were synthesized according to the procedures reported earlier [30,35]. Binary mixtures were prepared in sealed aluminum pans, heated to the isotropic phase, and ultrasonicated. The quality of the mixing was assessed by means of high-resolution calorimetry. More information regarding this preparation procedure, calorimetric studies, and also measurements of splay and bend elastic constants can be found in [31].

Molecular calculations predict a distribution of molecular shapes characterized by two broad peaks with maxima corresponding to an extended conformer (*trans* conformer) with an average angle between the mesogenic units of around 120° and a hairpin-shaped conformer (*cis* conformer) with an internal average angle around 30°. For high values of the nematic order parameter the most extended conformers are stabilized at the expense of the less extended conformers [1,21,34]. Figure 1 shows the chemical structures of the component compounds together with a schematic representation of the two main conformers for both dimers. The mean-square dipole moment is given by the averaged vector sum of the constituent dipole moments associated with the nitrile groups for CB7CB (∼4 D), and the two C-F bonds and nitrile group for the case of FFO9OCB (∼2.25 D). As can be appreciated, extended orientationally averaged conformers will contribute very differently to the permittivity component along the director ($\varepsilon_{||}$), with a zero mean-square dipole in the case of CB7CB and a nonzero component in the case of the nonsymmetric FFO9OCB. On the other hand, in both cases the hairpin conformers make a large contribution to the value of $\varepsilon_{||}$. Regardless of the configuration for both dimers there will be a nonzero transverse dipolar contribution to the perpendicular component of the permittivity ($\varepsilon_{\perp}$), which will depend on the average angle between the terminal groups. For the N_{TB} phase "parallel" and "perpendicular" refer to the helix axis.

In Fig. 2 we present both components of the static dielectric permittivity for three mixtures (CB7CB mole fractions: 0.21, 0.48, and 0.82) together with the corresponding values for the two pure compounds. The measurements were taken using an Agilent Precision LRC meter E4890A and Instec cells of 8 μm thickness with antiparallel planar rubbing. Samples were held on a hot stage (TMSG-600) and temperature controller (TMS-93) from Linkam. The perpendicular component $\varepsilon_{\perp}$ was obtained directly using harmonic probe fields of low

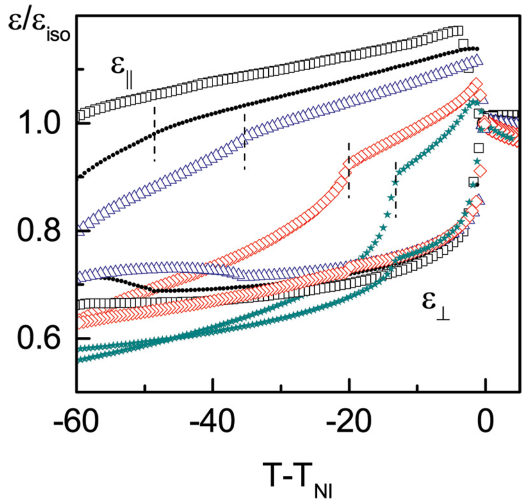

FIG. 2. Temperature dependence of the static permittivity of the two pure compounds and the three mixtures: (□) FFO9OCB; (●) $X_{CB7CB} = 0.21$; (△) $X_{CB7CB} = 0.48$; (◇) $X_{CB7CB} = 0.82$; (☆) CB7CB. Discontinuous lines correspond to the phase transition N_{TB}-N.

amplitude, 0.5 V_{rms}, well below the threshold voltage of the Fréedericksz transition. On the other hand, the parallel component $\varepsilon_{||}$ was measured by applying voltages well above the transition, which align the director parallel to the electric field. We have chosen 5 kHz as most convenient for the aligning field frequency [6]. As can be observed for all the samples, the behavior at the I-N transition is as expected for materials with positive dielectric anisotropy: $\varepsilon_{\perp}$ decreases and $\varepsilon_{||}$ increases. On further lowering the temperature, $\varepsilon_{\perp}$ is gradually stabilized in a very similar way, reflecting the increase of orientational order and the subtle effect that changes in the conformational distribution can exert on the averaged transverse component of the molecular dipole moment. However, the behavior of the parallel component strongly depends on the symmetric or nonsymmetric structure of the dimers. The aforementioned initial increase in the parallel permittivity on lowering the temperature at the I-N transition for CB7CB can only be explained by the slight stabilization of hairpin conformers, which carry a large longitudinal dipole moment, as opposed to the very broad distribution of molecular conformers in the isotropic phase [34]. After the initial increase, the parallel permittivity rapidly decreases in the nematic phase on further reducing the temperature. This behavior suggests a significant reduction of the average mean-square molecular dipole moment as the orientational order of the phase increases. Molecular calculations for CB7CB using a continuous torsional potential [1] for the connecting methylene chain showed that the increase of orientational order produces a progressive increase of the population of the more extended conformers with zero longitudinal dipole moment at the expense of the hairpin-shaped ones, which is in agreement with the observed temperature dependence of $\varepsilon_{||}$. Such changes in the conformational distribution seem to be common for liquid crystal dimers subject to a nematic potential [34]. On entering the N_{TB} phase, the continuous decrease of both components of the permittivity is accelerated, and at low temperatures there is even a sign reversal in the dielectric anisotropy from positive to negative.

For the nonsymmetric FFO9OCB dimer, the behavior is slightly different. The parallel component also decreases as the temperature is reduced but less drastically than for CB7CB; this observation is related to the nonzero value of the average dipole moment of the extended conformers [30]. This case is intermediate between the two extremes: The CBnCB family has two equal terminal groups, and no net longitudinal dipole component for extended conformers, while in the CBOnO.Py family [28,29] only one of the terminal groups has a significant dipole moment. In the latter case, the static permittivity is similar to the monomers of the nCB family, showing a continuous increase as temperature decreases. Interestingly, the static permittivity of the mixtures reveals the adequacy of the model for the interpretation of the dielectric results. $\varepsilon_{||}$ behaves in between the tendencies exhibited by both pure compounds, smoothly approaching from one to the other depending on the mole fraction. This is evidence that the contribution of the net longitudinal dipole of the extended nonsymmetric dimer hinders the drastic reduction of $\varepsilon_{||}$ seen for CB7CB and implies a higher value of the dielectric anisotropy. Also noteworthy is the behavior of $\varepsilon_{\perp}$ at the N-N_{TB} transition: While there is a decrease in the value for CB7CB, that of the mixtures shows an appreciable increase which can be explained in terms of the growth of the conical angle and the contribution of a net longitudinal dipole moment.

The analysis of the frequency-dependent dielectric permittivity for the mixtures in the N and N_{TB} phases will give information on the molecular orientational dynamics. In order to cover the whole frequency range 10^{-2}–1.8×10^{9} Hz and properly characterize the dielectric spectra of the materials, three different analyzers are needed: These are AlphaA from Novocontrol, HP4192A, and HP4291A. High-frequency dielectric measurements require the utilization of cells with untreated metal electrodes, which in our setup consists of a parallel plate capacitor made of two circular gold-plated brass electrodes with a 5-mm diameter separated by 50-μm-thick silica spacers.

For pure materials, the usual alignment achieved spontaneously in these cells with gold electrodes is a random planar alignment; i.e., the director is perpendicular to the probe measuring electric field. For materials having a positive dielectric anisotropy, it is possible to switch in the nematic phase the alignment to homeotropic (director along the field direction) with a suitable bias field. For the mixture studied, although having a positive dielectric anisotropy, the director alignment in the gold-electrode cells was not as described above. Since it is not possible to view the sample in the dielectric cell, assessment of the alignment was made by making the appropriate capacitance measurements, and then fitting these to the Havriliak-Negami function [see Eq. (3)]. From the fitting it is possible to determine the extrapolated zero-frequency permittivity, and compare this with values measured in glass cells at low frequency, for which the alignment can be checked visually. Thus, although the dielectric spectrum obtained for the mixture in the gold-electrode cells exhibited some distinctive features of the expected planar alignment, it was not perfect. Similarly, on application of a bias field the final aligned state was not a perfect homeotropic state. We found that by gentle shearing, the degree of homeotropic alignment could be increased, but even the best aligned samples had an extrapolated value for the zero-frequency parallel permittivity about 10% less than that expected from separate low-frequency measurements. Thus we term the state measured as "quasihomeotropic," but for the purposes of analyzing the dynamics probed along the parallel axis of the permittivity, the degree of alignment was satisfactory.

The sample was placed at the end of a coaxial line and a modified HP16091A coaxial test fixture was used as the sample holder and then held in a Novocontrol cryostat, which screens the system. Dielectric measurements were performed on cooling with different temperature steps being stabilized to ±20 mK. However, it should be noted that due to the time required to perform low-frequency scans down to 10^{-2} Hz with the AlphaA analyzer, only a few temperatures were measured in this low-frequency range below 40 °C, and will only be used for a preliminary analysis of the glass transition dynamics where they become relevant.

The frequency dependence of the real, $\varepsilon'(\omega)$, and imaginary, $\varepsilon''(\omega)$, parts of the quasihomeotropic dielectric permittivity components are given in Fig. 3 for temperatures in (b) the nematic, and (c) the twist-bend nematic phases together with (a) a three-dimensional plot of the dielectric losses vs temperature and frequency. Although in the isotropic phase

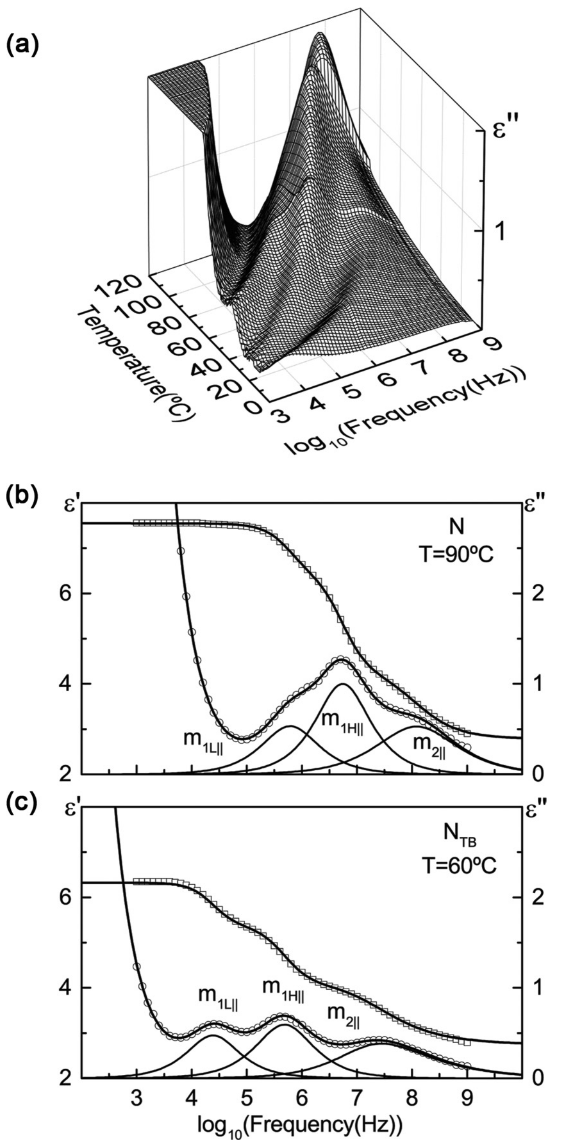

FIG. 3. Mixture with 0.48 mole fraction of CB7CB. (a) Three-dimensional plot of the dielectric losses vs temperature and logarithm of the frequency. Frequency dependence of ε' (□) and ε'' (○) (b) in the *N* phase, and (c) in the N_{TB} phase. In (b,c) solid lines are fits to Eq. (3).

there is only one mode, in both nematic phases the dielectric permittivity shows three relaxations, as in other nonsymmetric dimers [11,28,29] and in particular as in FFO9OCB [30]. The interpretation of such previous results required the development of a suitable theoretical model that is worth recalling here. Stocchero *et al.* [34] proposed a dynamic model based on the time-scale separation between the motion of the mesogenic units and the fast relaxation of the flexible chain. The original model of Maier-Saupe [36] for the dielectric relaxation of a dipolar molecule in a nematic potential was a two-state model representing the two orientations of a dipole along the director axis. In the case of the model of Stocchero *et al.* the resulting potential presents four deep wells corresponding to the four stable states of the dimer with the terminal groups parallel or antiparallel to the director. Such a potential provides the basis of the kinetic model for nematic dimers which considers that molecular reorientation occurs via a two-step process involving the individual orientational relaxation of the mesogenic units with different rates: $k_i^{T\to C}$ (rate coefficient for the reorientation of the rigid unit *i* from the *trans* to the *cis* configuration) and $k_i^{C\to T}$ (inverse process). Note that reorientations (end-over-end processes) of the connected dipolar groups are considered to be individual, but not independent, because of the correlation imposed by the flexible spacer and accounted for by the conformational distribution through the detailed balance equation $P_T^{eq}k_i^{T\to C} = P_C^{eq}k_i^{C\to T}$ [34], where P_T^{eq} and P_C^{eq} are the equilibrium populations of the *trans* and *cis* configurations, respectively. Whole molecular reorientation is excluded, since the energy barrier for the simultaneous rotation of both units is too high and results in a nonsignificant transition rate [34]. As order increases, calculation showed that the four wells become deeper but the barriers are still much smaller for the individual flip-flops than for the whole molecular reorientation. While the dynamics are determined by the energy barriers between the states, the dielectric strength of the relaxations are determined by the relative equilibrium populations of the orientational states.

For symmetric dimers the flipping rates of both units are equal and the resulting dipole moment correlation function

$$C_{||}(t) = 4\langle\mu_{||}\rangle^2 P_C^{eq}\exp(-2k^{C\to T}t), \qquad (1)$$

has a monoexponential decay, and so only a single low-frequency absorption, which, as has been shown for CB7CB and CB9CB [6,11], can be detected at frequencies corresponding to those of the intermediate frequency relaxation observed here and whose strength depends on the conformational distribution. On the other hand, for nonsymmetric dimers, relaxation rates would be different, and, depending on the shape and dipole moments of each unit, a variety of frequency relaxation profiles is predicted. In the case of FFO9OCB and assuming a relationship between dipole moments of both units given by $\langle\mu_{||}\rangle_{\mathrm{FF}} \approx 1/2\langle\mu\rangle_{||\mathrm{CN}}$, the model leads to the correlation function

$$\begin{aligned} C_{||}(t) = {} & \tfrac{1}{4}\langle\mu_{||}\rangle^2_{\mathrm{CN}}\big(P_T^{eq} - 3P_C^{eq}\big)^2\exp(-2k_Bt) \\ & + 4\langle\mu_{||}\rangle^2_{\mathrm{CN}}P_C^{eq}P_T^{eq}\exp(-2k_At), \end{aligned} \qquad (2)$$

where $k_A = \frac{1}{2}(k_A^{T\to C} + k_A^{C\to T})$ (*A* stands for the unit containing the CN group) and $k_B = 2(P_C^{eq}k_B^{C\to T}) = 2(P_T^{eq}k_B^{T\to C})$ (*B* stands for the unit containing the FF group). Equation (2) entails the emergence of an additional lower-frequency relaxation mode. Both low-frequency processes are related to the individual flip-flop motions of the units, and dielectric strengths are determined by equilibrium population their of the conformers [30,34]. Experimental results for FFO9OCB clearly confirm [30] such model's prediction. Accordingly, we associate the three dielectric relaxations observed for the mixture to (i) a superposition of the precessional motion of the dipolar groups around the director and the rotation around the long axis at the high-frequency branch of the spectrum (m_2) and (ii) the end-over-end reorientation of the dipolar groups parallel to the director at low frequencies (m_{1L} and m_{1H}) [34]. It is evident that the mixture shows a behavior resembling that of nonsymmetric dimers, with the appearance of a third dielectric mode at low frequencies, that in this case results from the fluorinated group reorientations.

The dielectric strengths of m_{1L} and m_{1H} for nonsymmetric dimers are predicted to depend on the conformational population distribution and on the relative value of the dipole moments of both terminal groups. Although the precise temperature dependence is intricate, the usual trend [11,28,29] is that the strength of the lower-frequency mode (m_{1L}) increases while that of m_{1H} decreases when the temperature is reduced as found for FFO9OCB [30]. Despite the similarity of the dielectric spectra of the mixture with that of FFO9OCB, the contribution of the symmetric CB7CB is clear when comparing the much higher strength of the m_{1H} mode with respect to that of pure FFO9OCB, as this mode can be associated with the reorientation of the nitrile groups of both dimers. In order to describe accurately the behavior of the mixture, the spectra for each temperature have been analyzed by fitting each relaxation mode according to the Havriliak-Negami function through the empirical relationship

$$\begin{aligned}\varepsilon(\omega) &= \varepsilon'(\omega) - i\varepsilon''(\omega)\\ &= \sum_k \frac{\Delta\varepsilon_k}{[1+(i\omega\tau_k)^{\alpha_k}]^{\beta_k}} - \frac{i\sigma_{\mathrm{dc}}}{\omega\varepsilon_0} + \varepsilon_\infty,\end{aligned} \tag{3}$$

where ε_∞ is the extrapolated high-frequency permittivity, $\Delta\varepsilon_k$ is the strength of the corresponding relaxation mode, and σ_{dc} is the dc conductivity. The relaxation time τ_k is related to the frequency of maximum loss through the parameters α_k and β_k, which describe the width and the asymmetry of the relaxation spectra, respectively ($\alpha = \beta = 1$ corresponds to a simple Debye-like process). The two low-frequency modes have a near-Debye shape in both mesophases and the high-frequency one is broader and asymmetric (having a Cole-Davidson shape with α about 0.8 and β ranging from 0.7 to 0.6). Dielectric strengths for each relaxation are given as a function of temperature in Fig. 4. The strength of the high-frequency mode m_2 in the N phase shows a decrease as the temperature decreases. On the other hand, the strengths of the two low-frequency modes, m_{1L} and m_{1H}, are correlated: while that of m_{1H} decreases, the strength of m_{1L} increases as temperature decreases in the N phase. This is the same trend observed for the corresponding modes for FFO9OCB [30]. The strengths of the three modes exhibit small jumps at the N-N_{TB} phase transition, but a proper quantitative analysis is not possible because the achieved alignment is not perfect. In fact we think that in a perfect parallel alignment $\Delta\varepsilon_2$ should be slightly smaller, taking into account the value obtained for FFO9OCB [30], and the strengths of the low-frequency modes slightly higher; the jumps at the transition downwards are provoked by the appearance of the tilt. What is interesting is the general trend: $\Delta\varepsilon_{1H}$ decreases while $\Delta\varepsilon_{1L}$ tends to saturate. It is important to recall that, even if the alignment were perfect, the precise analysis of the temperature dependence would be complicated since it involves both the temperature evolution of the population of the different conformers and the relative value of the dipoles in the terminal mesogenic units [28–30,34]. The frequency dependence of the modes can be determined over a broad temperature range, and as can be observed in Fig. 5 its temperature dependence in the N phase is similar to that found for FFO9OCB. Remarkably, at the N-N_{TB} phase transition the frequencies remain almost unaltered, compatible with a weakly first order phase transition. The two low-frequency modes follow the Arrhenius law in the N phase with activation energies of 85 kJ mol^{-1} (m_{1L}) and 70 kJ mol^{-1} (m_{1H}). At the higher temperatures in the N_{TB} phase, the low-frequency modes also follow the Arrhenius law with activation energies slightly larger, namely, 115 and 91 kJ mol^{-1}, respectively. However, in line with the glass transition detected by calorimetry at $-6\,^\circ$C [31], on reducing the temperature further there is a slowing down of the dynamics as the glassy state is approached, strongly deviating from the Arrhenius behavior. For this temperature range, Fig. 5 shows, superimposed, the corresponding fitting to the VFT (Vogel-Fulcher-Tammann) temperature-dependent relationship,

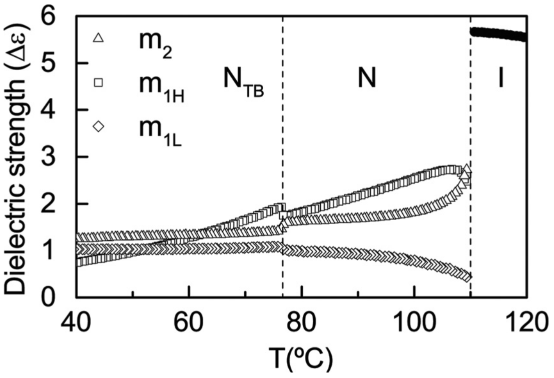

FIG. 4. Mixture with 0.48 mole fraction of CB7CB. Dielectric strength of the relaxation modes vs temperature: (●) isotropic phase; (△) m_2; (□) m_{1H}; (◇) m_{1L}.

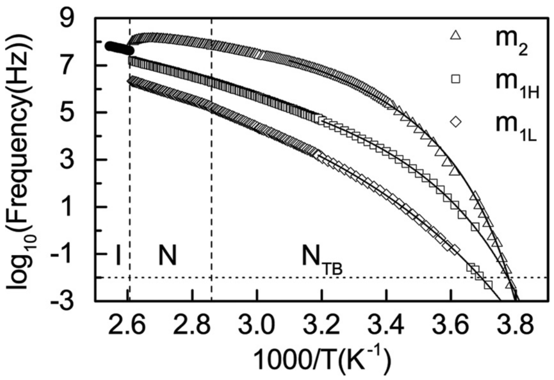

FIG. 5. Mixture with 0.48 mole fraction of CB7CB. Arrhenius plot of the frequency of the relaxation modes: (●) isotropic phase; (△) m_2; (□) m_{1H}; (◇) m_{1L}. Solid lines are fits to the VFT law, Eq. (4).

$$f_k = \frac{\omega_k}{2\pi} = f_{k0}\exp\left[\frac{B}{T-T_0}\right], \tag{4}$$

where f_{k0}, B, and T_0 are fitting parameters. The first important observation is that the m_{1H} mode seems to merge with m_2, in the same way as happens with the analogous m_1 and m_2 for CB7CB on approaching the glassy N_{TB} phase [2]. However, at least in our frequency-temperature window, m_{1L} evolves separately. For dielectric relaxation, a glass transition (known as a dynamic glass transition) is obtained when the characteristic relaxation frequency reaches 10^{-2} Hz. In Fig. 5

we can see how this value corresponds to the same temperature for m_2 and m_{1H} (around $-10\,^{\circ}$C) while it is reached at a slightly higher temperature for m_{1L} (around $-6\,^{\circ}$C). This implies that, from a dielectric point of view, two glass transition temperatures involving different molecular motions are present; the lower-temperature glass transition due to the dynamic disorder of the cyanobiphenyl group and that at higher temperatures attributed to the fluorinated group reorientations. In the latter case, the nematic environment at these low temperatures makes the steric interactions of each group much stronger, hindering the reorientations and increasing the required thermal energy. Accordingly, the associated glass transition temperature is higher than for the cyanobiphenyl group [37]. However, the analysis of the dynamics at this double glass transition is beyond the scope of this paper and needs to be confirmed by other experimental techniques and thoroughly examined with more detailed models [2].

III. SUMMARY

In our opinion the most interesting aspect of our results is that we have been able to study the dielectric spectra for a nonsymmetric dimer exhibiting the N_{TB} phase. We demonstrate that in a mixture containing a nonsymmetric element with an adequate molecular dipole the spectra resemble those of the nonsymmetric component by exhibiting three relaxation processes. The spectra can be satisfactorily explained in terms of the theoretical model for dielectric relaxation in liquid crystal dimers proposed by Stocchero *et al.* [34]. Recently, a study of the dielectric spectra of a six-component mixture, denoted KA(0.2) (three symmetric and three nonsymmetric dimers) in the N and N_{TB} phases was reported, attributing m_{1L} to whole molecule end-over-end rotation of cybotactic groups [38]. Interestingly, although x-ray studies in symmetric dimers such as CB9CB [33] also suggest the presence of domains, our dielectric results of this material [6] show a single relaxation process at frequencies similar to those of m_{1H} as predicted by Stocchero's model. In light of our previous studies and those presented here, we believe that the low-frequency mode described for the KA(0.2) mixture could be attributed to the contribution of the individual reorientation of the mesogenic units of the nonsymmetric compounds constituting the sample. Remarkably, in our mixture we could follow the dielectric modes over a very broad frequency-temperature range both in the N and N_{TB} phases. From a dielectric point of view, both nematic phases exhibit the same molecular active modes, with a similar behavior (only small changes in the strength, related to the director tilt, and in the activation energies) and the molecular environment, nematic or twist-bend nematic, scarcely affects the dielectric properties. However, as the mixture shows a glass transition, when reducing the temperature the molecular modes seem to become increasingly collective as already described for CB7CB [2].

ACKNOWLEDGMENTS

The authors are grateful for financial support from the MICINN Project No. MAT2015-66208-C3-2-P, and from the Eusko Jaurlaritza-Gobierno Vasco Project No. GI/IT-449-10. The authors also acknowledge the recognition from the Generalitat de Catalunya of GRPFM as Emergent Research Group (2009-SGR-1243). N.S. thanks the Alexander von Humboldt Foundation for support from a Postdoctoral Research Fellowship.

---

[1] M. Cestari, S. Diez-Berart, D. A. Dunmur, A. Ferrarini, M. R. de la Fuente, D. J. B. Jackson, D. O. López, G. R. Luckhurst, M. A. Pérez-Jubindo, R. M. Richardson, J. Salud, B. A. Timimi, and H. Zimmermann, Phys. Rev. E **84**, 031704 (2011).

[2] D. O. López, N. Sebastian, M. R. de la Fuente, J. C. Martínez-García, J. Salud, M. A. Pérez-Jubindo, S. Diez-Berart, D. A. Dunmur, and G. R. Luckhurst, J. Chem. Phys. **137**, 034502 (2012).

[3] D. Cheng, J. H. Porada, J. B. Hooper, A. Klittnick, Y. Shen, M. R. Tuchband, E. Korblova, D. Bedrov, D. M. Walba, M. A. Glaser, J. E. MacClennan, and N. A. Clark, Proc. Natl. Acad. Sci. USA **110**, 15931 (2013).

[4] V. Borsch, Y. K. Kim, J. Xiang, M. Gao, A. Jákli, V. P. Panov, J. K. Vij, C. T. Imrie, M. G. Tamba, G. H. Mehl, and O. D. Lavrentovich, Nat. Commun. **4**, 2635 (2013).

[5] V. P. Panov, R. Balachandran, J. K. Vij, M. G. Tamba, A. Kohlmeier, and G. H. Mehl, Appl. Phys. Lett. **101**, 234106 (2012).

[6] B. Robles-Hernández, N. Sebastián, M. R. de la Fuente, D. O. López, S. Diez-Berart, J. Salud, M. B. Ros, D. A. Dunmur, G. R. Luckhurst, and B. A. Timimi, Phys. Rev. E **92**, 062505 (2015).

[7] V. P. Panov, M. Nagaraj, J. K. Vij, Y. P. Panarin, A. Kohlmeier, M. G. Tamba, R. A. Lewis, and G. H. Mehl, Phys. Rev. Lett. **105**, 167801 (2010).

[8] P. A. Henderson and C. T. Imrie, Liq. Cryst. **38**, 1407 (2011).

[9] C. S. P. Tripathi, P. Losada-Pérez, C. Glorieux, A. Kohlmeier, M. G. Tamba, G. H. Mehl, and J. Leys, Phys. Rev. E **84**, 041707 (2011).

[10] M. Sepelj, A. Lesac, S. Baumeister, S. Diele, H. L. Nguyen, and D. W. Bruce, J. Mater. Chem. **17**, 1154 (2007).

[11] D. A. Dunmur, G. R. Luckhurst, M. R. de la Fuente, S. Diez, and M. A. Peréz-Jubindo, J. Chem. Phys. **115**, 8681 (2001).

[12] C. Meyer, G. R. Luckhurst, and I. Dozov, Phys. Rev. Lett. **111**, 067801 (2013).

[13] C. Meyer, G. R. Luckhurst, and I. Dozov, J. Mater. Chem. C **3**, 318 (2015).

[14] D. A. Dunmur, M. R. de la Fuente, M. A. Perez-Jubindo, and S. Diez, Liq. Cryst. **37**, 723 (2010).

[15] D. A. Dunmur, M. Cestari, S. Diez-Berart, A. Ferrarini, M. R. de la Fuente, D. J. B. Jackson, D. O. López, G. R. Luckhurst, M. A. Pérez-Jubindo, R. M. Richardson, J. Salud, B. A. Timimi, and H. Zimmermann, *Presented at the 23rd International Liquid Crystal Conference, Kraków, Poland, July 11–16, 2010*, Oral 60 (unpublished).

[16] R. J. Mandle, E. J. Davis, C. C. A. Voll, C. T. Archbold, J. W. Goodby, and S. J. Cowling, Liq. Cryst. **42**, 688 (2015).

[17] R. J. Mandle, E. J. Davis, C. T. Archbold, C. C. A. Voll, J. L. Andrews, S. J. Cowling, and J. W. Goodby, Chemistry **21**, 8158 (2015).

[18] Z. Ahmed, C. Welch, and G. H. Mehl, RSC Adv. **5**, 93513 (2015).

[19] E. Gorecka, N. Vaupotič, A. Zep, D. Pociecha, J. Yoshioka, J. Yamamoto, and H. Takezoe, Angew. Chem., Int. Ed. **54**, 10155 (2015).

[20] A. Zep, S. Aya, K. Aihara, K. Ema, D. Pociecha, K. Madrak, P. Bernatowicz, and H. Takezoe, J. Mater. Chem. C **1**, 46 (2013).

[21] M. Cestari, E. Frezza, A. Ferrarini, and G. R. Luckhurst, J. Mater. Chem. **21**, 12303 (2011).

[22] I. Dozov, Europhys. Lett. **56**, 247 (2001).

[23] R. B. Meyer, in *Molecular Fluids*, edited by R. Balian and G. Weill (Gordon and Breach, New York, 1976).

[24] S. M. Shamid, S. Dhakal, and J. V. Selinger, Phys. Rev. E **87**, 052503 (2013).

[25] R. Memmer, Liq. Cryst. **29**, 483 (2002).

[26] C. Greco and A. Ferrarini, Phys. Rev. Lett. **115**, 147801 (2015).

[27] N. Vaupotič, S. Curk, M. A. Osipov, M. Čepič, H. Takezoe, and E. Gorecka, Phys. Rev. E **93**, 022704 (2016).

[28] N. Sebastián, M. R. de la Fuente, D. O. López, M. A. Pérez-Jubindo, J. Salud, S. Diez-Berart, and M. B. Ros, J. Phys. Chem. B **115**, 9766 (2011).

[29] N. Sebastián, M. R. de la Fuente, D. O. López, M. A. Pérez-Jubindo, J. Salud, and M. B. Ros, J. Phys. Chem. B **117**, 14486 (2013).

[30] N. Sebastián, D. O. López, B. Robles-Hernández, M. R. de la Fuente, J. Salud, M. A. Pérez-Jubindo, D. A. Dunmur, G. R. Luckhurst, and D. J. B. Jackson, Phys. Chem. Chem. Phys. **16**, 21391 (2014).

[31] D. O. López, B. Robles-Hernández, J. Salud, M. R. de la Fuente, N. Sebastián, S. Diez-Berart, X. Jaen, D. A. Dunmur, and G. R. Luckhurst, Phys. Chem. Chem. Phys. **18**, 4394 (2016).

[32] K. Adlem, M. Čopič, G. R. Luckhurst, A. Martelj, O. Parri, R. M. Richardson, B. D. Snow, B. A. Timimi, R. P. Tuffin, and D. Wilkies, Phys. Rev. E **88**, 022503 (2013).

[33] E. Ramou, Z. Ahmed, C. Welch, P. K. Karahaliou, and G. H. Mehl, Soft Matter **12**, 888 (2016).

[34] M. Stocchero, A. Ferrarini, G. J. Moro, D. A. Dunmur, and G. R. Luckhurst, J. Chem. Phys. **121**, 8079 (2004).

[35] P. J. Barnes, A. G. Douglass, S. K. Heeks, and G. R. Luckhurst, Liq. Cryst. **13**, 603 (1993).

[36] G. Meier and A. Saupe, Mol. Cryst. **1**, 515 (1966).

[37] S. Diez-Berart, D. O. López, J. Salud, J. A. Diego, J. Sellarés, B. Robles-Hernández, M. R. de la Fuente, and M. B. Ros, Materials **8**, 3334 (2015).

[38] R. R. Ribeiro de Almeida, C. Zhang, O. Parri, S. N. Sprunt, and A. Jákli, Liq. Cryst. **41**, 1661 (2014).